

# Techniques for Deriving Optimal Bondlines for Athermal Bonded Mounts

James J. Herbert

Ball Aerospace & Technologies Corp., Boulder, CO 80301

## Abstract

Deriving the optimal bondline thickness for an athermal bondline depends on many factors. An optimum bondline is defined as one that produces zero radial stress at the optic/adhesive interface. A review of the current equations in use and a new non-linear equation defined for optic mounts over larger temperature ranges is included. An assessment of sensitivities around the optimum bondline thickness is discussed. Also, guidelines for do's and don'ts in athermal optics mounts is included.

**Keywords:** bonds, adhesive, athermal, elastomer

Nomenclature			
$\alpha$	coefficient of thermal expansion	T	temperature
d	diameter	$\Delta T$	change of temperature
E	modulus of elasticity		
G	shear modulus	ave	subscript for average
$\varepsilon$	strain	b	subscript for bond
h	thickness of bond	c	subscript for lens cell
L	width of bond	nl	subscript for nonlinear
$K_{1c}$	fracture toughness	o	subscript for optic
$\sigma$	stress	$\theta$	subscript for tangential
P	load (lb/in)	r	subscript for radial
$\nu$	Poisson's ratio	ult	subscript for ultimate $\sigma$
$\tau$	shear stress	z	subscript for axial

## 1. Introduction

Much has been written over the years on athermal bonded mounts for optics. The idea of an adhesive making up the difference of the thermal strain between the lens housing and the optic is very appealing. It provides a continuous boundary condition for the optic, enabling a strong connection for harsh mechanical environments and a benign boundary for the optic, thus not disturbing surface figure. To make the lens and housing coexist with these attributes requires a certain bondline width. The precision of needed bondline increases over the larger thermal excursion and as the adhesive Poisson's ratio ( $\nu$ ) approaches 0.5. At least three equations currently exist for calculating the optimum bondline.

DeLuzio<sup>1</sup> derived an equation for an athermal bondline that accounts for the hydrostatic effect of the in-plane strains (axial and tangential) of the bond being essentially zero. This effect<sup>2</sup> magnifies the radial coefficient of thermal expansion (CTE) and the radial direction modulus of elasticity as Poisson's ratio approaches 0.5. The DeLuzio derivation can also be used to calculate radial stresses at the optic for non-optimal bondline thickness.

The next equation published is Bayar's<sup>3</sup> equation. This equation calculates the difference in CTEs of the various materials in the lens mount to arrive at the optimum bond thickness. It does not account for the hydrostatic Poisson's effect but is useful if the effective CTE of the adhesive can be obtained through test or analysis.

Another athermal bondline equation is the Muench equation<sup>4,5,6</sup>. Unfortunately, it exists in at least four different forms in published work with only reference 6 having it correct. The correct version of the equation will be discussed in this paper.

These equations do not address several issues that may, in many applications, significantly affect the accuracy of their results. Material nonlinearities play a big roll in deriving the optimum bondline over a large temperature range. Adhesive properties along with residual stresses from the adhesive cure are factors that should be considered. An assessment of the stress at the edge of the bond will also be discussed.

## 2.0 Equation Development

The bonded optic mount considered in this paper assumes a round optic bonded to a cell or housing. The equations for this optic system will use cylindrical coordinates as defined in the cross-sectional view in Figure 1. The objective of this exercise is to define the optimum bondline thickness around the optic producing zero radial stress or only a slight compression at the optic perimeter.

Examples in this study will use a 2.835 inch diameter optic. The example optic cells will include: Germanium and fused silica for the optics, RTV and a ductile epoxy for the bonds, and titanium, aluminum, and invar for the cells. The material properties are shown in Appendix A.

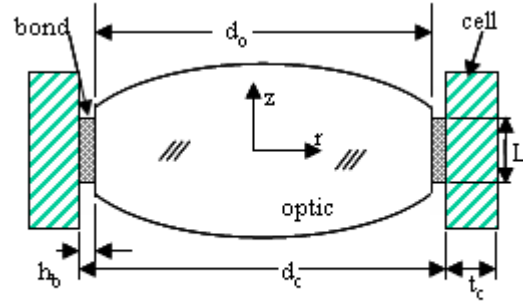


Figure 1 Typical athermal lens mount

The stress-strain relationship for the bond is defined in equation (1) with the assumption of small strains.

$$\begin{pmatrix} \sigma_{b,r} \\ \sigma_{b,\theta} \\ \sigma_{b,z} \\ \tau_{b,rz} \end{pmatrix} = \frac{E_b}{(1 + \nu_b) \cdot (1 - 2 \cdot \nu_b)} \cdot \begin{bmatrix} (1 - \nu_b) & \nu_b & \nu_b & 0 \\ \nu_b & (1 - \nu_b) & \nu_b & 0 \\ \nu_b & \nu_b & (1 - \nu_b) & 0 \\ 0 & 0 & 0 & \frac{1 - 2 \cdot \nu_b}{2} \end{bmatrix} \cdot \begin{pmatrix} \varepsilon_{b,r} - \alpha_b \cdot \Delta T \\ \varepsilon_{b,\theta} - \alpha_b \cdot \Delta T \\ \varepsilon_{b,z} - \alpha_b \cdot \Delta T \\ \gamma_{b,rz} \end{pmatrix} \quad (1)$$

Also, it is assumed that the tangential stress is negligible and the stresses in the axial direction are only of concern in axial acceleration environments. Notice as Poisson's ratio approaches 0.5, the first term of the right hand side becomes singular. The adhesive becomes more incompressible or hydrostatic as Poisson's ratio approaches 0.5. The adhesive wants to maintain the same volume in this state but is restrained at the traction boundary of the adhesive interface with the optic and cell. The adhesive is trying to make up for this constraint at the free edges or traction-free boundary<sup>2</sup>. Solving for the adhesive stresses in the radial direction, we can examine this phenomenon:

$$\sigma_{b,r} = \frac{E_b}{(1 + \nu_b) \cdot (1 - 2 \cdot \nu_b)} \cdot \left[ (1 - \nu_b) \cdot \varepsilon_{b,r} + \nu_b \cdot (\varepsilon_{b,\theta} + \varepsilon_{b,z}) \right] - \frac{E_b \cdot \alpha_b \cdot \Delta T}{1 - 2 \cdot \nu_b} \quad (2)$$

The adhesive is generally much softer than the cell or the optic; thus, the in-plane adhesive strains,  $\varepsilon_\theta$  and  $\varepsilon_z$  are zero in the boundary of bondline and the adherends. Neglecting thermal effects, equation (2) reduces to a magnification factor for the radial adhesive modulus:

$$E_{b,eff} = \frac{1 - \nu_b}{(1 + \nu_b) \cdot (1 - 2 \cdot \nu_b)} \cdot E_b = M_E \cdot E_b \quad (3)$$

Now, returning to equation (2) and letting  $\sigma_r = 0$  for an athermal bondline:

$$0 = \frac{E_b}{(1 + \nu_b) \cdot (1 - 2 \cdot \nu_b)} \cdot (1 - \nu_b) \cdot \varepsilon_r - \frac{E_b \cdot \alpha_b \cdot \Delta T}{1 - 2 \cdot \nu_b} \quad (4)$$

Solving for radial strain in the adhesive  $\varepsilon_r$ :

$$\varepsilon_r = \alpha_b \cdot \frac{(1 + \nu_b) \cdot \Delta T}{1 - \nu_b} \quad (5)$$

Thus, the adhesive has a CTE magnification factor on radial strain of:

$$\alpha_{b,eff} = \frac{1 + \nu_b}{1 - \nu_b} \cdot \alpha_b = M_\alpha \cdot \alpha_b \tag{6}$$

Plots of these magnification factors are shown in Figure 2. The radial direction adhesive modulus increases dramatically as  $\nu$  approaches 0.5. This attribute increases the optic's sensitivity to radial stresses due to non-optimal bondlines. The CTE magnification could have a significant influence on the optimum bondline thickness. Further examining equation (1), notice the shear stresses and strains are not influenced by the hydrostatic effect. Since these magnifications are based strictly on analytical techniques, one must consider the aspect ratio (bond width, L versus radial bond thickness, h, i.e. L/h) of the bondline. Several papers<sup>7,8,9</sup> address the influence of bond shape factor on the Poisson's ratio magnification factor using either test or FEM techniques. Figures 3 and 4 are plots of bond aspect ratio correction factors generated from the curves or methodology in those references. These two aspect ratio corrections factors, one for the adhesive modulus and the other for the adhesive CTE, are multiplied times the Poisson's ratio magnification factors. The aspect ratio correction factors will be utilized throughout this paper.

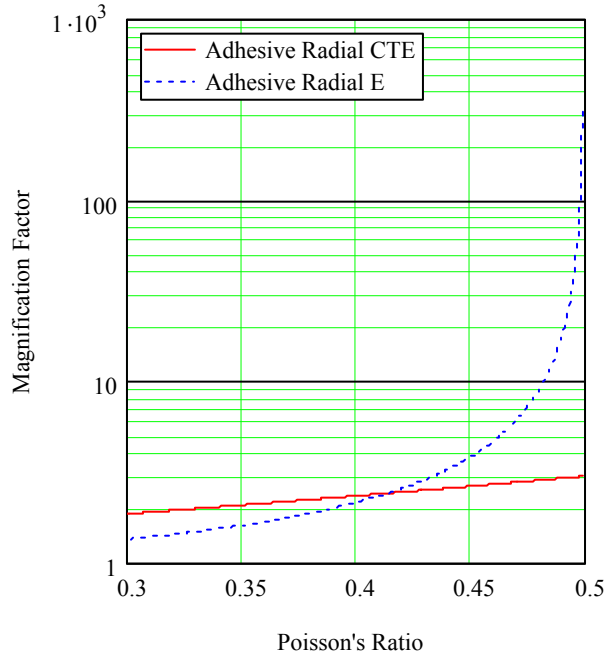


Figure 2 Poisson's Ratio Effect

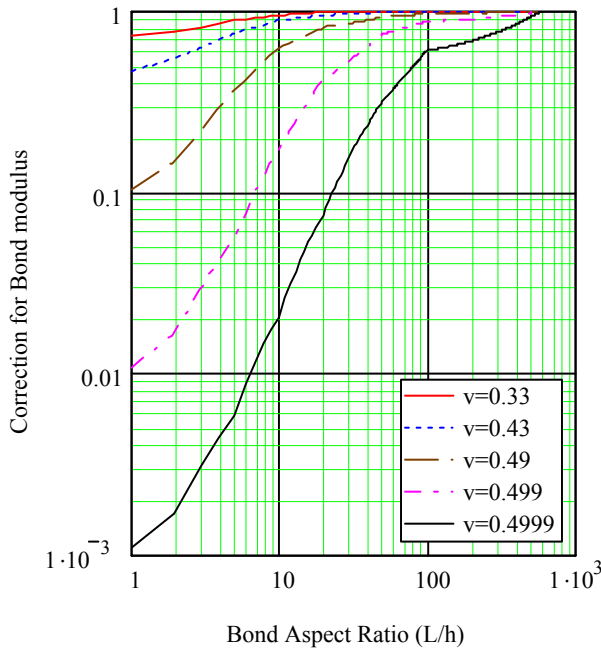


Figure 3 Aspect Ratio E correction

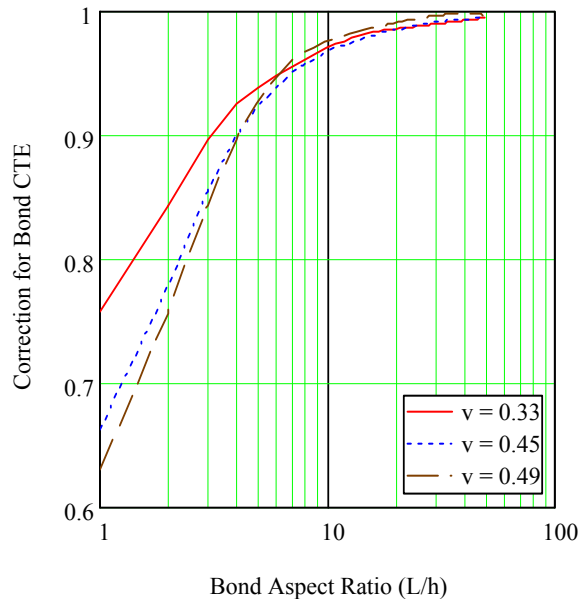


Figure 4 Aspect Ratio CTE Correction

## 2.1 Bayar's Equation

Bayar's is the simplest of the three equations described in the introduction. The equation is shown in equation (7) with terms described in Figure 1.

$$h_{\text{bayar}} = \frac{d_o \cdot (\alpha_c - \alpha_o)}{2 \cdot (\alpha_b - \alpha_c)} \quad (7)$$

This equation calculates the thermo-elastic distortion difference between the cell and the optic with the adhesive thermal-elastic distortion making up the difference. It is a useful, simple equation and can be used if the temperature range is relatively small and Poisson's ratio is not near 0.5. The CTEs used in this equation and any of the other linear athermal equations should be average CTEs derived from the assembly temperature of the lens and the expected operating temperature. In other words, this is the expected thermal strain of the material divided by the  $\Delta T$ .

One rule of thumb that is applicable for any of the bondline calculations is that the lens cell (also called the housing or bezel in many of the publications) must have a CTE greater than that of the optic, and the adhesive CTE must be greater than both the optic and the cell. More simply put:

$$\alpha_b > \alpha_c > \alpha_o \quad (8)$$

If this rule is violated, an optimum solution does not exist and will put the optic in tension. Tension must be avoided for optics composed of ceramics or glass susceptible to stress corrosion. Also, it is advantageous to use a softer adhesive for mounting optics to minimize stresses introduced into the optic. The strongest adhesive is not necessarily the best choice. Strength in the adhesive is usually not an issue with the mount; dimensional stability and stress in the optic are the overriding requirements.

The Bayar equation can be modified to account for the amplification of the adhesive CTE as Poisson's ratio increases by substituting equation (6) into equation (7). The aspect ratio also needs to be considered, but equation (9) is fairly accurate for thin bondlines ( $L/h > 10$ ).

$$h_{\text{bayar}} = \frac{d_o \cdot (\alpha_c - \alpha_o)}{2 \cdot \left( \frac{1 + \nu_b}{1 - \nu_b} \cdot \alpha_b - \alpha_c \right)} \quad (9)$$

## 2.2 Muench Equation

The Bayar equation is widely used in industry but another equation in the opto-mechanical world is the Muench<sup>10</sup> equation (10). Unfortunately this equation is victim to typos in other publications. In a conversation with Mr. Muench, he confirmed that the version shown here is correct and is valid for the entire range of Poisson's ratio. Mr. Muench also informed me that the equation was originally derived by Roel Vanbezoijen.

$$h_{\text{muench}} = \frac{d_o}{2} \cdot \frac{\alpha_c - \alpha_o}{\alpha_b - \alpha_c + \left( \alpha_b - \frac{\alpha_c + \alpha_o}{2} \right) \cdot \left( \frac{2}{1 - \nu_b} \cdot \nu_b \right)} \quad (10)$$

## 2.3 DeLuzio Equation

DeLuzio<sup>1</sup> derived this athermal equation in the late 1960's for Itek. Using equation (1) along with static equilibrium equations and linear strain displacement relationships, he derived equation (11) for an optimum bondline thickness.

$$h_{\text{deluzio}} = \frac{d_o}{2} \cdot \frac{1 - \nu_b}{1 + \nu_b} \cdot \frac{\alpha_c - \alpha_o}{\left( \alpha_b - \alpha_o \right) - \frac{(7 - 6 \cdot \nu_b) \cdot (\alpha_c - \alpha_o)}{4 \cdot (1 + \nu_b)}} \quad (11)$$

Figure 5 compares equations (9), (10), and (11) over the range of Poisson's ratios. Muench and DeLuzio equations track very closely but, the modified Bayar equation bondline is thinner due to the full CTE magnification. This example uses the Germanium lens in a titanium cell bonded with a ductile epoxy operating at 90 Kelvin. Figure 6 shows the effect of adding the CTE corrections factor from Figure 4 to these equations. All of the bonds get thicker due the lower corrected adhesive CTE. The aspect ratio in Figure 6 varies from 5 to about 8 with a 0.25" wide bondline.

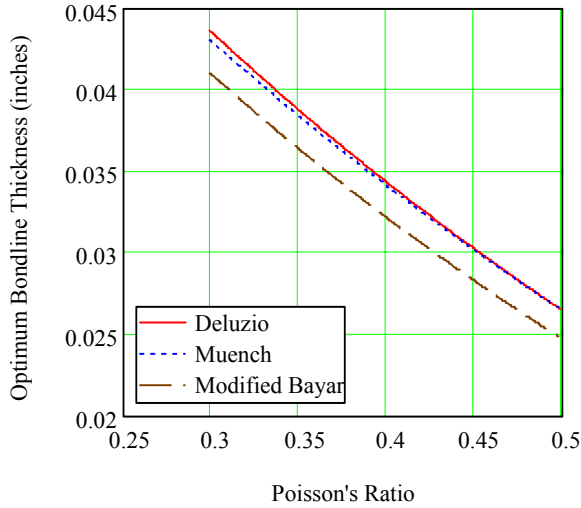


Figure 5 Athermal Equation Comparison

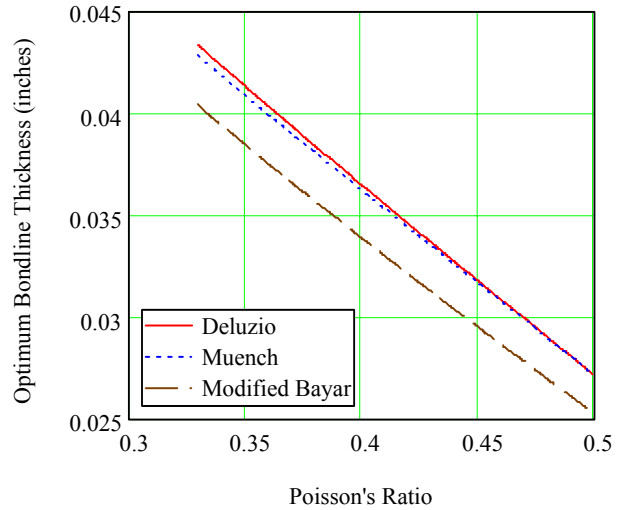


Fig.6 Equation w/CTE correction L=0.25"

Another equation of interest found earlier in the Deluzio paper, is a formulation for the radial stresses (12) at the optic/bond interface as a function of bondline thickness.

$$\sigma_{o,r} = \frac{E_b \cdot \Delta T}{4 \cdot (1 - 2 \cdot \nu_b) \cdot (1 + \nu_b)} \cdot \left[ \frac{-1}{\ln\left(\frac{r_2(h)}{r_o}\right)} + (10 - 8 \cdot \nu_b) \cdot \frac{r_2(h)^2}{r_2(h)^2 - r_o^2} \right] (\alpha_c - \alpha_o) + 4 \cdot (1 + \nu_b) \cdot (\alpha_o - \alpha_b) \quad (12)$$

where  $r_o = \frac{d_o}{2} \quad (13)$

$r_2(h) = \frac{d_o}{2} + h \quad (14)$

Using equation (12) instead of (10), the optimum thickness is found by where equation (12) crosses zero radial stress with thickness as a variable. This form of the equation can also be used to examine what tolerances are needed at the bondline to protect the optic from going into tension. In Figure 7, we look at an example between two different adhesives and cells using equation (12). The RTV example only goes to 150°K since its glass transition is at 145°K. The slope of the RTV line implies much greater sensitivity to non-optimum bondlines even though it has a much lower bulk modulus than the epoxy (100:1). But when the RTV modulus is corrected using the curves in Figure 3, the stresses are not nearly as sensitive. The epoxy mount is less sensitive to a non-optimum bondline than RTV before being corrected for aspect ratio. The epoxy slope bondline radial stress changes by a factor of two after it is corrected for its aspect ratio. The dramatic change of the slope of the RTV induced stresses probably explains how the industry has survived using soft elastomers and non-optimum bondlines. If the modulus aspect ratio correction was not true, we would have a lot more broken optics.

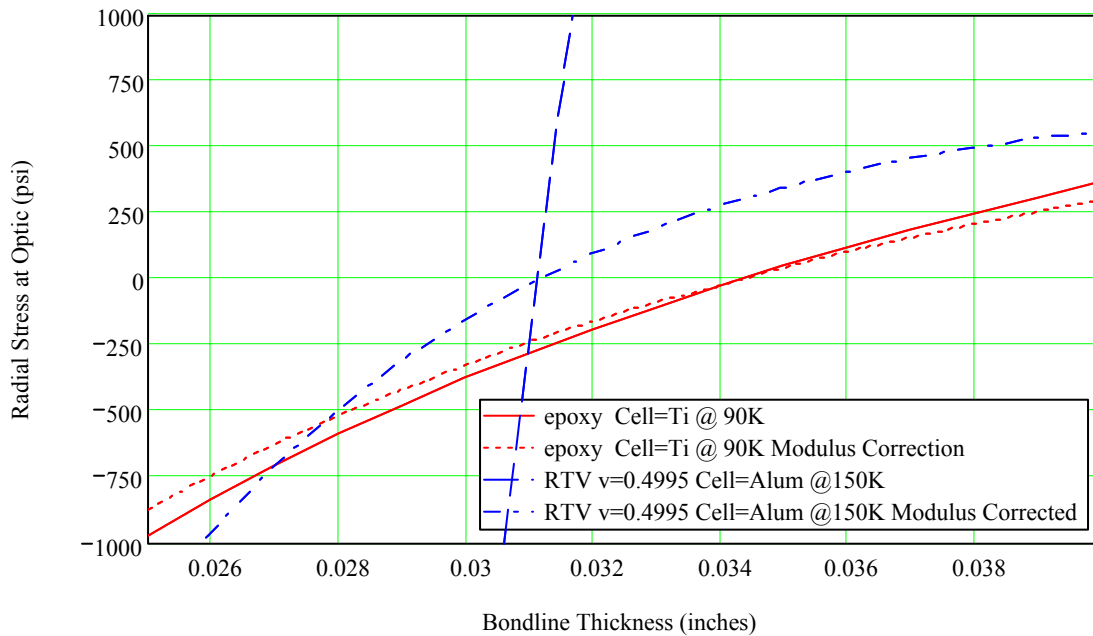


Figure 7 Bondline Sensitivity L=.25"

Figure 8 examines the influence of the aspect ratio correction using equation (12). The example lens is corrected for both E and CTE, thus flattening the radial stress curve and driving the optimum to the right for thicker bondlines. The corrected athermal bondline starts to converge with the original equation at aspect ratio higher than 10.

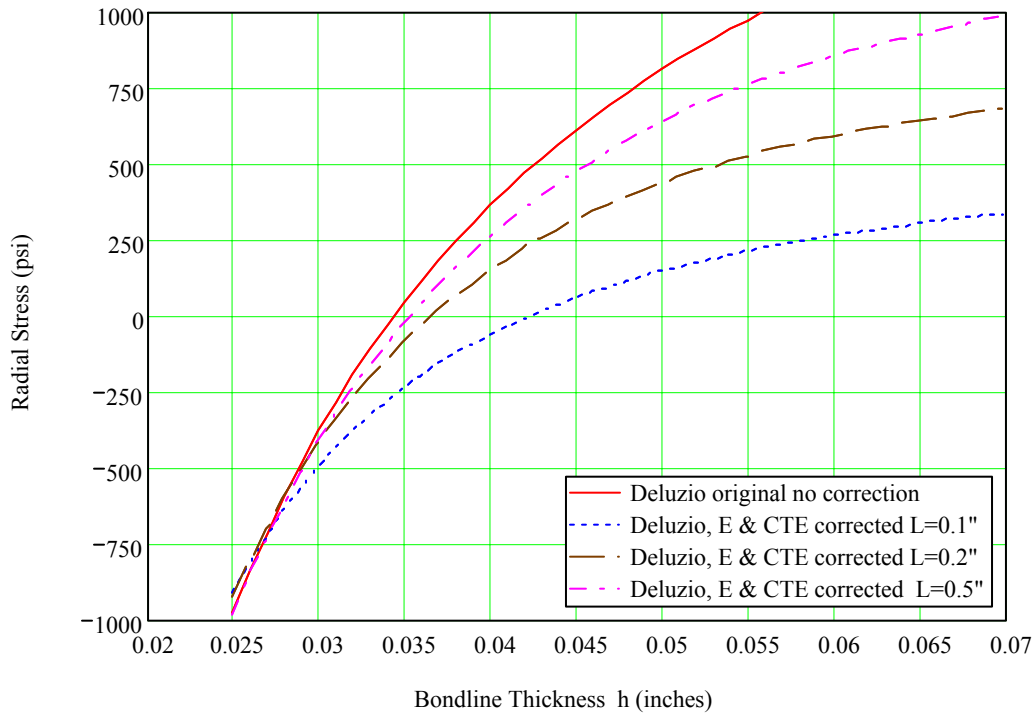


Fig. 8 Ge/Epoxy/Ti@90K E & CTE corrected

## 2.4 Nonlinear athermal equation

Over large temperature ranges, material properties of the cell, the optic, and especially the adhesive behave in a nonlinear fashion. Considering these nonlinear material properties, the solution to an optimum bondline becomes path dependent since the properties change independently from room temperature to operating temperature. Stepping down in temperature in much the same way as the actual optic does, a nonlinear optimal bondline can be found in a cumulative solution by rewriting equation (12) to include all of the material non-linearities. The CTEs of all the materials in equation (12) now need to be calculated using thermal strains as shown in equations (15),(16), and (17). We use numerical differentiation to approximate the instantaneous CTE at that point on the thermal path. The adhesive modulus and Poisson's ratio also change over temperature in equation (14).

$$\sigma_{o.r.nl}(h) = \sum_{T=293}^{90} \left[ \frac{E_b(T)}{4 \cdot (1 - 2 \cdot \nu_b(T)) \cdot (1 + \nu_b(T))} \cdot \left[ \frac{-1}{\ln\left(\frac{r_2(h)}{r_1}\right)} \dots \right] \cdot (\alpha_c(T) - \alpha_o(T)) \dots \right] \left[ \begin{array}{l} + (10 - 8 \cdot \nu_b(T)) \cdot \frac{r_2(h)^2}{r_2(h)^2 - r_1^2} \\ + 4 \cdot (1 + \nu_b(T)) \cdot (\alpha_o(T) - \alpha_b(T)) \end{array} \right] \quad (14)$$

$$\alpha_c(T) = \varepsilon_c(T - 1) - \varepsilon_c(T) \quad (15)$$

$$\alpha_o(T) = \varepsilon_o(T - 1) - \varepsilon_o(T) \quad (16)$$

$$\alpha_b(T) = \varepsilon_b(T - 1) - \varepsilon_b(T) \quad (17)$$

Figure 9 compares the linear and nonlinear solutions. The optimum bondline varies from the linear solution by 0.003". Not using a nonlinear equation when faced with a large temperature range results in more stress at the bondline and an increase in optic surface distortion. Aspect ratio correction once again flattens and moves the optimum thickness to the right.

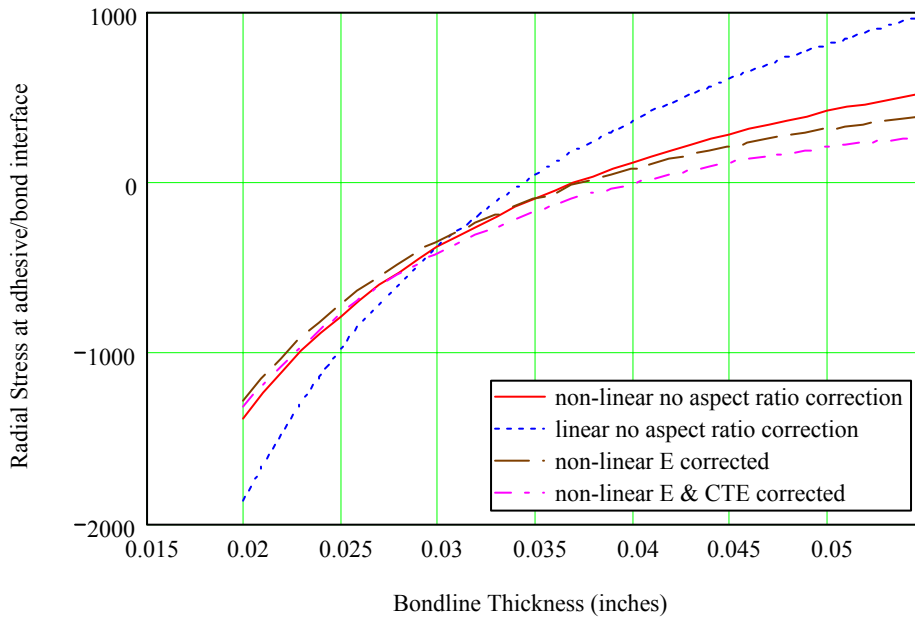


Fig 9 Linear vs Nonlinear Ge/Ep/Ti 90K

### 3.0 Other environments

Radial stresses in transient thermal cases is another scenario commonly encountered yet seldom, if ever tracked. The optic tends to lag the cell temperature when going through a thermal excursion. During warm up (i.e. the optic is colder than the cell) the optic tends to be in tension causing the worst case. Equation (14) can be easily modified to account for this condition by increasing the cell's temperature by some delta in equation (15). Figure 10 shows the effect on radial stress when the optic lags the cell temperature by 20 degrees (K). The nonlinear equation gives insight into the worst case temperature, in this case at 210°K. Both of the plots in Figure 10 have been corrected for the aspect ratio. The fused silica with an Invar cell is interesting because the fused silica has an inverted thermal strain curve (Figure A.2) and actually generates more stress even though both materials have very low CTEs. The Ge/Ep/Ti mount has h=0.048 inches and a bond width of 0.2 inches. The Fused Silica/Ep/Invar mount has h=0.022 inches and also a width of 0.2 inches.

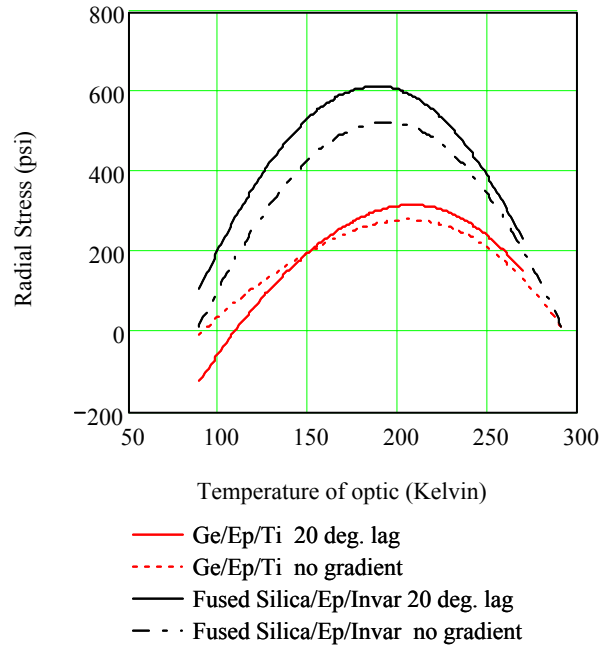


Fig 10 Stresses vs temperature range

### 3.1 Inertial Environments

Stresses at the edge of the bondline should also be examined. FEM techniques, while widely used, do a poor job with adhesive bondlines especially with a thermal environment<sup>10</sup>. The problem involves a singularity that appears at the end of the bondline due to different material properties and the difficulty of resolving the shear stress. Many papers have been written on this issue using complex closed form solutions or some non-linear FEM technique. An easy way to view this issue is by using a Hart-Smith<sup>11</sup> equation to calculate adhesive strain at the end of the bondline. This equation is based on a one dimensional adhesive strain model. Because it is one-dimensional, it does not include the bond CTE or Poisson's ratio. That said, the equation is adequate for assessing stresses unless dealing with very fragile optics that have strengths less than 1000 psi. The Hart-Smith equation can be broken down into two parts, equation (18) for mechanical or acceleration loads and equation (19) for thermal mismatch stresses.

$$\tau_a = \tau_{ave} \cdot \lambda \cdot \frac{L}{2} \cdot \left[ \frac{\left( \frac{E_c \cdot t_c - E_o \cdot t_o}{E_c \cdot t_c + E_o \cdot t_o} \right) \cdot \tanh\left(\lambda \cdot \frac{L}{2}\right) + \frac{1}{\tanh\left(\lambda \cdot \frac{L}{2}\right)}} \right] \quad (18)$$

$$\tau_a = \frac{\lambda \cdot (\alpha_o - \alpha_c) \cdot \Delta T}{\frac{1}{E_c \cdot t_c} + \frac{1}{E_o \cdot t_o}} \cdot \tanh\left(\lambda \cdot \frac{L}{2}\right) \quad (19)$$

where ..

$$\lambda = \sqrt{\frac{G_a}{h} \cdot \left( \frac{1}{E_c \cdot t_c} + \frac{1}{E_o \cdot t_o} \right)} \quad (20)$$

$$\tau_{ave} = \frac{P}{L} \quad (21)$$

In our example Germanium optic, the thermal induced adhesive shear stress at the edge of the bondline is 41 psi and 32 psi for a 100g axial load.



#### 4.0 Optic Strength

Optic strength is often an issue when analyzing bonded optics. The optic is often a brittle material, either a ceramic or glass, that has weak tension strength. Trying to obtain strength for these materials is sometimes not easy and requires expensive testing. If the fracture toughness and crack growth data are available, using the techniques outlined by Doyle and Kahan<sup>12</sup> is a good approach. In lieu of that, a conservative shortcut equation<sup>13</sup> (22) can be used if only the fracture toughness of the material is known and anticipated flaw size at the surface of the bond area is known or can be estimated.

$$\sigma_{\text{ult}} = \frac{K_{1c}}{4\sqrt{\pi \cdot 3 \cdot \text{flaw}}} \quad (22)$$

As can be seen in this equation, strength is very dependent on the quality of the bond surface for these brittle materials. It is recommended that this surface is polished and kept as dry as possible during bonding. Fracture toughness and strength properties degrade in the presence of moisture. The equation also accommodates the general guideline of using 3 times the visible flaw size<sup>14</sup> in strength calculations. This is because the actual flaw may be up to three times its visible size.

As mentioned before, if the optic material tension allowable is less than 1000 psi, a higher fidelity optic mount may be needed to both match CTE between the cell and the optic and provide additional compliance in the radial direction.

Another good rule of thumb to minimize optic stresses and surface distortions is to limit the bond edge no closer than 0.05 inches from the edges on the optic. If the bondline approaches the optic front surface/edge interface, higher stresses will be induced into the optic front (optical) surface. When it comes to bonds, controlling the adhesive to specific regions along the optic radial edge (as shown in Figure 1) will result in better overall performance of the bond and the optic. The use of bonding dams or some other system to control excess adhesive is recommended.

#### 5.0 Adhesive Properties

Accurate adhesive properties are needed to calculate optimum athermal bondlines. Vendor data usually lack the necessary material properties, especially over a larger temperature range. Accurate CTE, shear modulus, and Poisson's ratio are needed over the specified thermal range. The bulk adhesive CTE data can be obtained using a fairly simple test, but the  $\nu$  and the shear modulus tend to be more difficult to obtain. Shear modulus data from published sources tend to be very high because it is derived from tests meant for much stiffer adhesives and higher strain rates. Because thermal environment tends to occur at a low strain rate, the type of test needed is a thick adherend test<sup>15</sup> or a torsional test<sup>16</sup> run at slower strain rates. Published shear modulus data normally come from a dynamic mechanic analyzer (bulk, clamped three point bend) or tension dog-bone specimen run at much higher strain rates and involve other nonlinearities. The strength of the adhesive is usually not a concern on a continuous bonded mount.

The glass transition temperature of the adhesive must be accounted for to ensure a good athermal optic. A bonded optic mount should not be allowed to go through the adhesive glass transition temperature either when it is approaching its operating range or in its operating range. The adhesive's properties dramatically change as the glass transition temperature is approached and render the linear athermal equations invalid. The bonded optic should stay on one side or the other of the adhesive glass transition temperature.

Shrinkage is another adhesive property of interest. If the adhesive cure shrinkage and elastic modulus is low, it is usually not a large contributor to optic surface distortion. For an adhesive with a higher modulus and cure shrinkage, a FEM should be used to assess the shrinkage stress at the optic/adhesive interface. If the residual shrinkage stresses are of concern, the bondline can be adjusted by biasing the adhesive thickness using equation (12) or (14).

Attention should also be paid to the adhesive cure temperature. The bonded optic should be cured to at least as high as the optic is going to operate since the adhesive modulus and CTE may permanently change (cure more completely) with an elevated cure thus adding more dimensional stability to overall mount over its life. Curing at room temperature for an extended length of time before an elevated temperature exposure may help reduce some these effects.

## 6.0 Summary

In summary, the DeLuzio equation (11) or Muench equation (10) can be used for most athermal optimum bondline calculations. The standard Bayar equation can be used for mounts with bond aspect near unity. Over large temperature ranges, the nonlinear equation (14) should be used. The following is a summary of other guidelines discussed in this paper.

1. The athermal mount must follow this rule:  $\alpha_b > \alpha_c > \alpha_o$
2. Keep bonds away from the surface interfaces of the optic.
3. Optics made from brittle materials need polished surfaces at the bondline to maximize strength.
4. Thermal lag of the optic should be investigated. It may be the worst case.
5. Nonlinear effects should be considered over large temperature ranges and/or unusual material properties.
6. Keep the bonded optics from going through the adhesive glass transition regions.
7. Dimensional tolerances should be biased to keep the optic in compression.
8. The bonding surface should be as dry as possible prior to bonding
9. On powered optics, lines of action may not go the center of gravity.
10. The aspect ratio corrections should be used for bondlines with a ratio less than 10.

### References:

1. **A. J. DeLuzio, "Optimization of elastomer thickness for edge mounted mirrors subject to uniform temperature changes" Itek Technical Report ATR 68-16 August 1968**
2. **Anees Ahmad, Handbook of Optomechanical Engineering, p.292 CRC 1997**
3. **Mete Bayar, "Lens barrel opto-mechanical design principles" Optical Eng. Vol 20 No.2**
4. **Daniel Vukobratovich, "Bonded Mounts for small Cryogenic Optics" SPIE Vol 4131**
5. **Paul Yoder, Mounting Optics in Optical Instruments, p. 72 SPIE Press 2002**
6. **K. Doyle, G. Michels, V. Genberg, "Athermal design of nearly incompressible bonds" , SPIE Vol. 4771 (35), Seattle, WA, July, 2002**
7. **A. Hatheway, "Analysis of adhesive bonds in optics", SPIE Vol. 1998 Optomechanical Design (1993)**
8. **T. Mast, et al, "Elastometric Lens Mount", SPIE Vol. 3355 March 1998**
9. **G. Michels,., V. Genberg, K. Doyle, "Finite element modeling of nearly incompressible bonds", SPIE Vol. 4771 (34), Seattle, WA, July 2002**
10. **MIL-HDBK-17-3F, p.6-46**
11. **Hart Smith NASA CR-112235 "Adhesive-Bonded Double Lap Shear Joints"**
12. **K. Doyle, M. Kahan "Design Strength of Optical Glass", SPIE Vol. 5178(4), San Diego, CA, Aug 2003**
13. **Schott: "TIE-33: Design Strength of optical glass & ZERODUR"**
14. **SSP 30560 "Glass, Window, and Ceramic Structural Design and Verification Requirements - International Space Station Program**
15. **ASTM D 3983 - 98**
16. **L.J. Hart-Smith, "Differences between adhesive behavior in test coupons and structural joints", Douglas Paper 7066 1981**

### Acknowledgements

The author would like to acknowledge the contributions of co-workers including Tom Kampe, Glenn Taudien, Holden Chase, Hiwot Molla, Phil Quigley, and Tom Yarnell in overcoming the challenging optomechanical problems on recent programs. I would also like to thank Joe Girard, Duffy Morales, and Andy Sievers in the preparation of this paper.

## Appendix A Material Properties

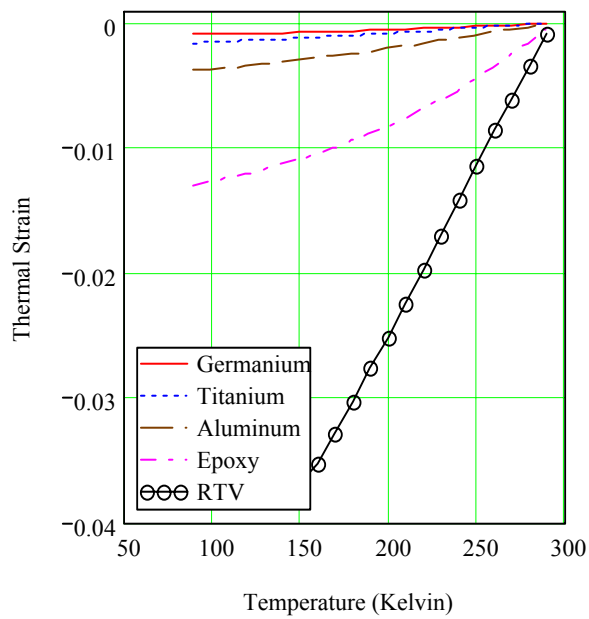


Figure A.1 Thermal Strain

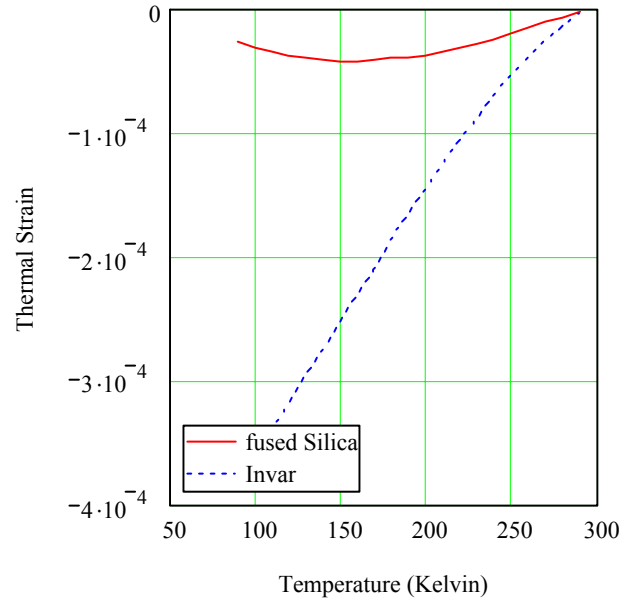


Figure A.2 Thermal Strain

Table A.1 Material Properties			
	E (psi)	$\nu$	CTE (ppm/K)
fused silica	9.70E+06	0.17	0.13 (90K)
Germanium	1.50E+07	0.28	4.5 (90K)
RTV	500 (293K) 1700 (150K)	0.4995	260
Epoxy	30000 (150K) 45000 (90K)	0.43 (293K) 0.4 (90K)	76 (150K) 64 (90K)
Aluminum	1.00E+07	0.33	18.54 (90K) 20.61 (150K)
Invar	2.20E+07	0.259	1.8 (90K)
Titanium	1.60E+07	0.33	7.72 (90K) 8.33 (150K)

Note: Parameters in ( ) are integrated averages 293°K to operating